

GAZİ

JOURNAL OF ENGINEERING SCIENCES

## Comparative Analysis of Composite Buildings Produced in National and International Standards

Serkan Etli<sup>a</sup>, Melek Akgül<sup>\*b</sup>

Submitted: 20.01.2023 Revised: 04.05.2023 Accepted: 05.05.2023 doi:10.30855/gmbd.0705063

### ABSTRACT

**Keywords:** Composite moment resisting frame, Concrete filled steel tube column, Incremental dynamic analysis, Nonlinear pushover analysis, Seismic behavior factor

<sup>a</sup> Munzur University  
, Dep. of Emergency Aid  
and Disaster Management,  
062000 - Tunceli, Türkiye  
Orcid: 0000-0003-3093-4106  
e mail: melekakgul@munzur.edu.tr

<sup>b\*</sup> Munzur University,  
Tunceli Vocational Schools,  
62000 - Tunceli, Turkey  
Orcid: 0000-0001-8815-3762

\*Corresponding author:  
melekakgul@munzur.edu.tr

Composite moment resisting frame buildings with 5-, 10-, 15- and 20-story concrete filled steel tube columns and composite beams were modelled. The buildings are designed according to Turkish Code for Design and Construction of Steel Structures-2016 (TCDCSS-2016) and Türkiye Building Earthquake Code-2018 (TBEC-2018) regulations at high ductility levels. The design of the DCH structures was designed in ZC ground for a 0.79 g PGA. While choosing the design location, it is assumed that the construction will be made in a region between the North Anatolian fault line and the East Anatolian fault line, that is, in a region with high earthquake risk. Within the scope of the study, SeismoStruct [1] software was used during the design and performance evaluation of the structures. Nonlinear static push and incremental dynamic analyses were used. Uniform and triangular load distributions were adopted in the PO analysis, and 16 earthquake ground motions were used in the dynamic analysis. The effect of story number on the seismic behavior of CMRFs was investigated using nonlinear analysis results. Accordingly, variation in lateral response, overstrength factors, ductility, and section capacity change of members for CMRF structures were presented. In addition, a mutual evaluation was made with the performance parameters obtained from previous studies with similar geometries.

## Ulusal ve Uluslararası Standartlarda Üretilen Kompozit Binaların Karşılaştırmalı Analizi

### ÖZ

5-, 10-, 15- ve 20 katlı binalar beton dolgulu çelik tüp kolonlu ve kompozit kirişli moment aktaran çerçeve binalar modellenmiştir. Binalar yüksek süneklik seviyelerinde TCDCSS - 2016 ve TBEC-2018 yönetmeliğine göre tasarlanmıştır. DCH yapılarının tasarımı, 0.79 g PGA için ZC zeminde tasarlanmıştır. Tasarım yeri seçilirken, inşaatın Kuzey Anadolu fay hattı ile Doğu Anadolu fay hattı arasında kalan bir bölgede, yani deprem riskinin yüksek olduğu bir bölgede yapılacağı varsayılmıştır. Çalışma kapsamında yapıların tasarımı ve performans değerlendirmesi yapılırken SeismoStruct [1] yazılımı kullanılmıştır. Doğrusal olmayan statik itme ve artımlı dinamik analizler kullanılmıştır. PO analizinde düzgün ve üçgen yük dağılımları kullanılmıştır. Dinamik analizde 16 deprem yer hareketi kullanılmıştır. Kat sayısının CMRF'lerin sismik davranışı üzerindeki etkisi doğrusal olmayan analiz sonuçları kullanılarak incelenmiştir. Buna göre, CMRF yapıları için elemanların yanal tepkisindeki değişim, aşırı dayanım faktörleri, süneklik ve kesit kapasitesi değişimi sunulmuştur. Ayrıca benzer geometrilere sahip önceki çalışmalardan elde edilen yapıların performans parametreleri ile karşılıklı bir değerlendirme yapılmıştır.

**Anahtar Kelimeler:** Kompozit moment aktaran çerçeve, Beton dolgulu çelik tüp kolon, Artımsal dinamik analiz, Doğrusal olmayan statik itme analiz, Sismik davranış faktörü

## 1. Introduction

As the design heights of the buildings increase, the need to use columns with high strength capacities increases, especially to absorb earthquake effects [2]. For steel structures, high strength in columns can be achieved by using steel material class with high yield strength and/or profiles selected as larger cross-sections. On the other hand, in a similar situation in reinforced concrete structures, higher capacity columns can be obtained by increasing the class and/or compressive strength of the concrete material used and again by increasing the cross section. It is also possible to benefit from the high yield strength of the steel obtained by forming a single section and the high compressive strength of the concrete. Among the sections that can be produced in this way, the most used and experimentally/theoretically studied concrete-filled steel tube (CFST) sections in the last century are the most used column elements (Figure 1) [3-7].



Figure 1. Some examples of buildings whose construction has been completed are in order from left to right, SEG plaza in Shenzhen, Ruifeng building in Hangzhou and Canton Tower [7]

The strength of columns, which are vertical loading members in both steel and reinforced concrete structures, can be made with designs that can be made without using relatively large cross-sectional areas. In other words, by using composite sections made of steel and concrete (or reinforced concrete), more suitable sections can be obtained, and the required capacity increase can be achieved. However, if only moment resisting frames (MRF) are used for design during the behavior of earthquake loads, it is necessary to limit the relative story drifts and secondary effects. In this case, by using composite columns in the design, the required stiffness and ductility can be achieved more effectively than steel and reinforced concrete systems. Considering the large axial force strength for the columns used in steel frames with central and eccentric braces, the required strength can be easily obtained by forming CFST columns profile [8-10].

Today, the use of composite profiles instead of reinforced concrete or steel profiles in elements with high compressive strength, which can meet the increasing axial pressures and have high ductility during element design, is more advantageous in terms of construction speed and economics, especially in high-rise buildings designs. It is known that the steel profile creates a continuous confinement effect in the concrete, especially when looking at the CFST column elements. On the other hand, it is expected that the strength and ductility of concrete will increase while CFST acts as a core within the element. In addition to all these positive effects, its location in the concrete core prevents local buckling of the steel profile [11,12].

Examining the nonlinear responses of earthquake resistant MRF systems, in which composite section elements are used during design, is important in terms of evaluating the advantages available in such systems. Non-linear analyzes were used in the studies on the design and performance evaluation of multi-story MRF, which consists of composite section column and beam elements, under the influence of earthquakes. In this analysis phase, it has been shown that the evaluation and identification of the member is very important in terms of convergence of the results to reality. Therefore, for an accurate

performance evaluation, column-beam junctions and related deformation conditions must be carefully evaluated and added to the system. In addition, in the study in which the natural vibration properties of a steel-concrete composite frame and its non-linear behavior under the effect of earthquakes were examined by making static and dynamic analyses, it was revealed that modelling techniques are important [13].

When the techniques of sectional elements in composite element modeling are examined, when the finite element method is applied in element-based studies, it can be modeled very closely. However, it is very difficult to define the number of elements formed and the surface interactions established between them. In structural systems, on the other hand, defining element sections as solids one by one is both time-consuming and difficult in terms of modeling technique. On the other hand, the number of elements that will occur in the system prolongs the analysis process considerably. On the other hand, modelling of these elements based on the loading system is important in terms of design, so the time to reach the solution is not effective. Therefore, the fiber cross-section model, which is an alternative to this technique and provides the opportunity to make sensitive analyses as well as being faster, seems to be a more practical method [11,12,14,16].

In the models examined within the scope of this study composite moment resisting frames (CMRF), the structural system consisting of square section (SHS) CFST columns, IPE steel beams and composite beams, which are in full interaction with the slab, were examined. 5-, 10-, 15- and 20-storey structures were designed as CMRF using the principles of the Regulation on Design, Calculation and Construction Principles of Steel Structures 2016 (TCDCCS-2016) [17] and the Turkish Building Earthquake Code 2018 (TBEC-2018) [18] on the seismic design. Static pushover analysis (PO) and incremental dynamic analysis (IDA) were used to obtain information on the earthquake performance of the buildings. The cross-sectional deformations of the loading system elements and the response of the system in terms of various parameters were evaluated. As a result, the performances of the buildings modelled within the scope of TBEC-2018 were examined comparatively with static and dynamic methods for a certain ground property. A flowchart of the method followed is presented in the Figure 2.

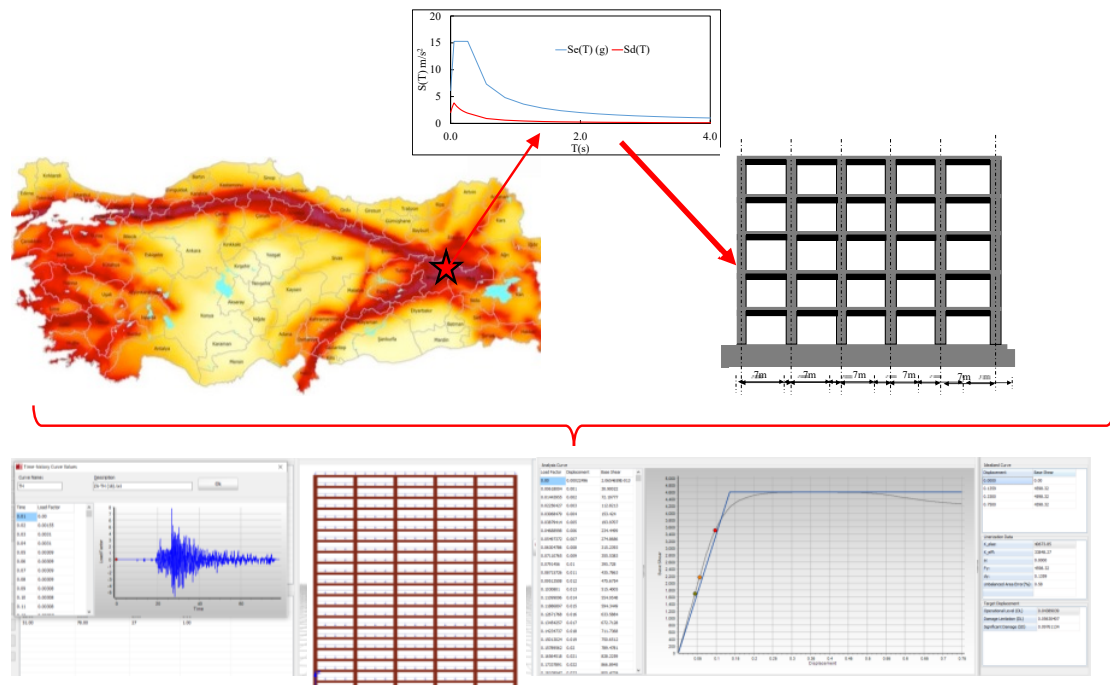


Figure 2. Flowchart of methodology

## 2. Example Structures

In the building designs, steel tube elements with SHS section and sections obtained by filling the cores with concrete suitable for the design were used in the column elements. These elements are composite columns defined as CFST section in the literature. Vertical and horizontal earthquake loads of beams

are calculated under static and dynamic design loads, and their sections are dimensioned to consist of IPE type steel section elements. In all MRF systems, designs have been made so that moment transfer occurs at the joint points of IPE frame beams and CFST columns and are included in the analysis (Figure 3). During the design, the flooring systems were made massive. It is included in the calculations as a cast-in-situ reinforced concrete slab system that can be accepted at the design stage with the full interaction of the floor slabs on the main beams. The anchorage of the columns in the foundation system is included in the calculations with the assumption of full support in both directions. The storey height of the CMRF structures is 2.65 m and the total height from the ground is 113.25, 26.5, 39.75 and 53 m for 5-, 10-, 15- and 20-storey structures, respectively. 5 openings in the x and y directions of the buildings modeled in CMRF structures and 7 m spans each are included in the design calculations. Therefore, the total width of the CMRF systems in the x and y directions is constant and is 35m (Figure 4). Seismic parameters are needed to design CMRF systems. For this reason, a location in Bingöl Province Kaloiva District Yeşilyurt Mahallesi (Latitude: 39.298011° Longitude: 41.014378°) was preferred in the design phase to carry out the design processes over a hypothetical location. For this geographical location, ZC, which is the soil conditions used in the systems to be compared with the literature, was chosen conditions. While steel class is S235 in structural system elements, concrete class is determined as C30/37 in the design. The analytical models used during the sizing of the structural elements of the building as CMRF are given in Figure 5. SeismoStruct [1] computer software was used in the design and performance evaluation and development of the analytical model (Figure 5). To take into account possible torsion effects in the direction calculated according to TBEC-2018 clause 4.5.10.2.b, an eccentricity of 5% of the floor length in the direction perpendicular to the earthquake direction is considered.

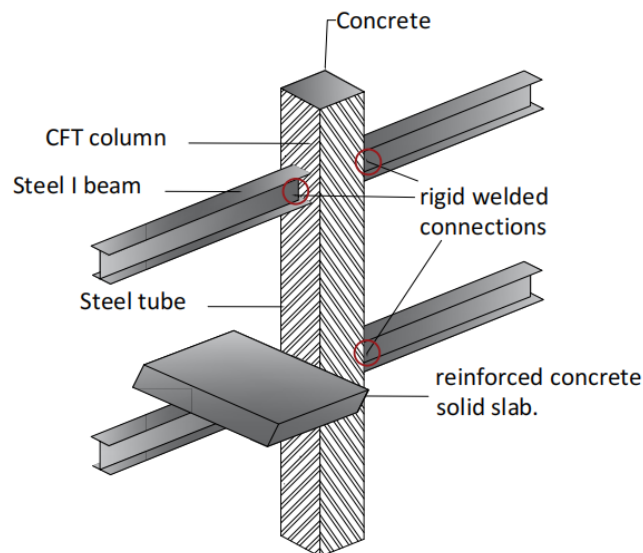


Figure 3. System view for MRF joint configuration.

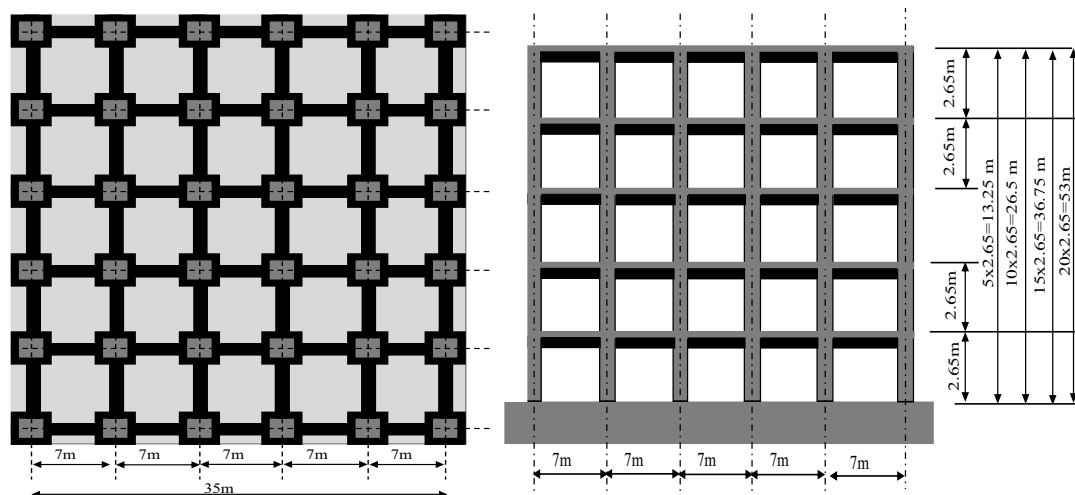


Figure 4. Schematic view of plane and elevation view

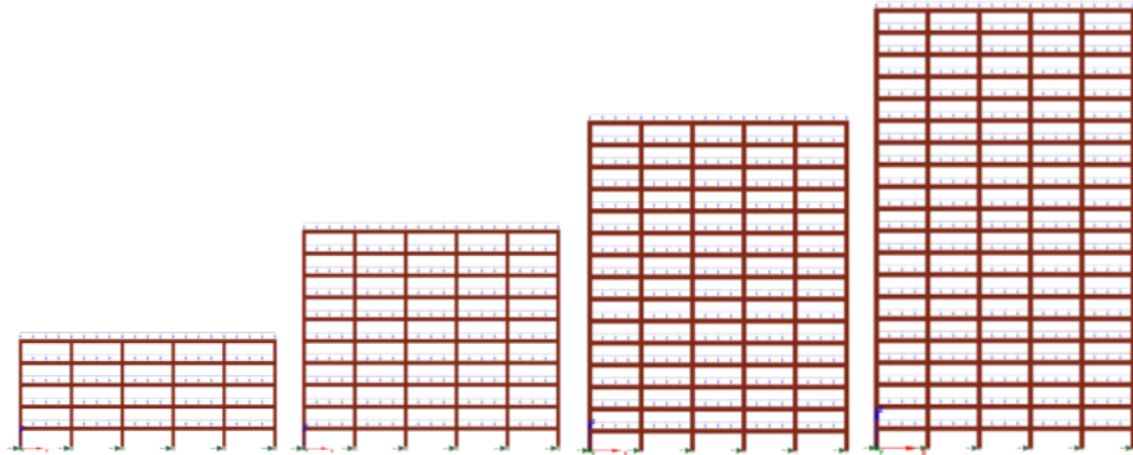


Figure 5. SeismoStruct program view of CMRFs

## 2.1. Structural design

During the design of the CMRF systems, the dimensioning of the sections and the section capacities were made in accordance with the TCDCSS-2016 and TBEC-2018 Regulations by using the loads acting on the beam and column elements in the system. In the CMRF design analysis, the SeismoStruct [1] computer software was evaluated in accordance with the relevant regulations and used in the analysis. The self-weights of the structural elements are calculated automatically by the program in line with the data entered the computer software and are considered in the analysis. During the seismic design analysis of the buildings, the dead load value was defined as  $3 \text{ kN/m}^2$  and was considered in the analyses. The live load was taken as  $2.0 \text{ kN/m}^2$ . To determine earthquake loads in seismic designs, it is necessary to obtain graphs of elastic design spectral accelerations. These data are taken from the relevant design regulations. In addition, the natural vibration period of the structure should be calculated. Within the scope of this study, the natural vibration period was calculated using Equation (2.2) given in TBEC-2018, and then the seismic forces were calculated according to the accelerations obtained from the elastic spectrum using the natural vibration period. For this reason, firstly, the calculations of the horizontal elastic design spectrum were made. For this purpose, the relevant spectrum was obtained based on the *DD-2* earthquake ground motion level, which has a 10% probability of exceedance in 50 years, and the local soil class *ZC*. On the other hand, information on spectral acceleration coefficients and ground effect coefficients should be determined in the creation of horizontal elastic design spectrum values. The data of the map spectral acceleration values were determined through the geographical location data selected for the construction sites of the design models and the Turkey Earthquake Hazard Maps [19]. Local ground effect coefficients were obtained based on local ground effect coefficients for local soil class and short period region and local ground effect coefficients for 1.0 second period according to TBEC-2018 Section 2.3.3. The damping ratio was taken as 5%. seismic design analysis. Using the Turkey Earthquake Hazard Maps [19], the short-term map spectral acceleration coefficient was read as  $SS= 1.947$ , and the map spectral acceleration coefficient for the 1.0 second period was read as  $S1= 0.514$ . The highest ground acceleration was obtained as  $PGA=0.791g$  and the highest ground speed as  $PGV=60.469 \text{ cm/s}$ . It is of great importance that the structural systems can serve the collapse prevention performance after severe earthquakes caused by continental plate tectonic movements. Compliance with the relevant regulations is of great importance, especially to minimize the material and moral damages that occur in earthquakes such as the 06.02.2023 Kahramanmaraş earthquake that occurred recently. Relevant design criteria are constantly updated in the literature by researchers and commissions in national and international standards. Comparative evaluation of the information contained in current international and national regulations is important in this respect. The designed buildings are evaluated as residential buildings, considering the damages and losses after the earthquakes in question. In addition, the general structural design coefficients used in such structures have been considered from the relevant sections of TBEC 2018.

In the study, the properties of the structural system were designed as composite beams consisting of CFST columns with high ductility and IPE section steel beams during the design phase. In accordance with this situation, according to Section 4.3.2.2 given in TBEC-2018, the behavior coefficient  $R$  and the

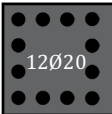
extreme resistance coefficient  $D$  will be used. In the selection of the relevant values,  $R$  and  $D$  column systems and steel structure systems, which are recommended to be used for the composite section, will be used. According to Table 4.1 given in TBEC-2018 for the properties of the structures, the coefficients of  $R=8$  and  $D=3$  given for buildings with steel frames with high ductility level and where all earthquake effects are carried by MRF systems are taken as basis. for these CMRFs. The General Analysis Method was used to calculate the required strengths of the structural elements, and the Design Method with Load and Strength Coefficients was used for dimensioning. As a requirement of this method, the axial and shear stiffnesses of all the elements of the lateral structural system (composite columns and frame beams in this study) and the bending stiffnesses of the frame beams were multiplied by one. According to TCDCSS-2016 6.2.3 0.8. The reduction coefficient applied to the bending stiffnesses of the composite columns was obtained as  $0.8 \times 0.8 = 0.64$  according to TCDCSS-2016 6.2.3(b) and 12.2.5(d). The natural vibration periods, total CMRF weights and base shear forces were calculated from SeismoStruct software. The values were given in Table 1.

Table 1. Design results

Parameter	5-story	10-story	15-story	20-story
Natural vibration periods (s)	0.677	1.440	1.595	2.131
Total CMRF weights (kN)	6484	13475.8	23376.5	32553.7
Base shear forces (kN)	770.7	792.4	1204.4	1237.5

According to the data obtained from the analysis results, no additional analysis was required, since no irregularity occurred in the plan and vertically in the analyzes made under the influence of the earthquake, and the CMRF structures were modeled to have a smooth geometry in plan and elevation. It was seen that the evaluation of the effective relative story drift ratio and secondary order effects coefficients provided the limit values defined in TBEC-2018 article 4.9. In addition, the seismic design features performed with composite beam and column elements with high ductility level and the seismic design analysis results show that the system provides the conditions for designing at high ductility level. Columns were designed in accordance with section 12.3.2 of the Design, Calculation and Construction Principles of Steel Structures (TCDCSS-2016) Regulation. The method used to calculate the column cross section involves using the axial force-bending moment interaction diagram. TCDCSS-2016 Table 12.5, which contains information about the plastic stress distribution method, was used to obtain this diagram. In addition, the limit condition  $N_{dm} \leq 0.40P_{no}$  for axial pressure force levels in composite columns specified in TBEC-2018 section 9.11.4.2 meets all CMRF systems.  $N_{dm}$  is defined as the maximum pressure force value obtained from the axial pressure forces calculated from the combined effect analysis in which vertical loads and earthquake loads are considered together (taking into account the live load reduction coefficients defined for live loads in TS 498 [20]).  $P_{no}$  is defined as the compressive strength of the composite section. During the CMRF seismic design, strong column weak beam design was applied at all beam-column joints and column-beam junctions for the analysis of each earthquake direction. Relevant details are given in TBEC-2018 9.11.2.2.

Table 2. Section and material properties of the structural members

ID	Beam	CFST Column (bxt mm)	Section details	Concrete	Structural Steel	Reinforcement
5-story	IPE 400	450x32		C30/37	S235	S420c
10-story	IPE 400	500x32				
15-story	IPE 500	650x40				
20-story	IPE 500	750x55				

The cross-sectional properties and material properties of composite columns and beams in CMRF structures after seismic analysis are presented in Table 2.

## 2.2. Nonlinear analytical models of the CMRF system

After the seismic design was completed in accordance with TCDCCS-2016 Regulation [17] and TBEC-2018 [18], the analyzes to obtain the nonlinear behavior of CMRF structures were carried out using SeismoStruct [1] computer software. Firstly, the analytical models were transformed into fiber cross-sectional elements during the design phase. In these elements, considering the material properties used, the new systems have been updated with element models with nonlinear behavior by taking advantage of previous studies. Thanks to the use of these element and material models, the software enables the analysis to be concluded by using the structural and geometric quadratic effects in all analyses. For the non-linear behavior of the composite columns and beams, models based on the bulk plastic behavior approach and represented in the software as predefined are used. In these modeling elements, sections divided into fiber elements were used to obtain the plastic behavior of the composite beams and columns in the model. In these models, the element section is divided along the element into the number of fiber elements specified by the designer in the section according to an algorithm in the software. In this way, it is assumed that the plastic behavior is propagated by the fiber elements in the element section and throughout the element. More importantly, it has been verified by the researchers that the element force-deformation distribution between the fiber parts of the concrete and steel sections forming the composite section is provided with sufficient accuracy by the software [5, 6, 11, 12, 21, 22]. The plastic behavior that occurs or is likely to occur in the entire element during the analysis is directly determined by the SeismoStruct software based on the material properties and model given by the designer in the software. Numerical models defined as ready-made in the software work with different assumptions by theorizing the results obtained from the literature during calculations. Moreover, during the definition of models and the use of analyzes, basic physical properties for these model elements, such as basic input parameters, section geometry, and uniaxial behavior, need to be defined in accordance with the models. CFST column members and composite beams are modeled as fiber cross-sections as shown in Figure 6 by the number of fibers specified in the software. The tiles were not considered directly in the analytical models. However, it is assumed that rigid diaphragms are formed at the floor level in each floor plane by defining the system. The vertical load combinations of dead and live loads calculated from the floors are defined as the system loads on the frame beams.

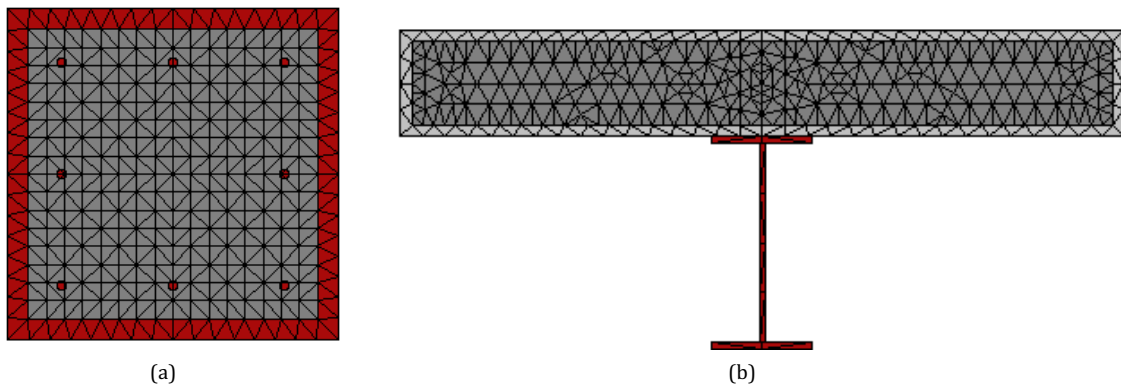
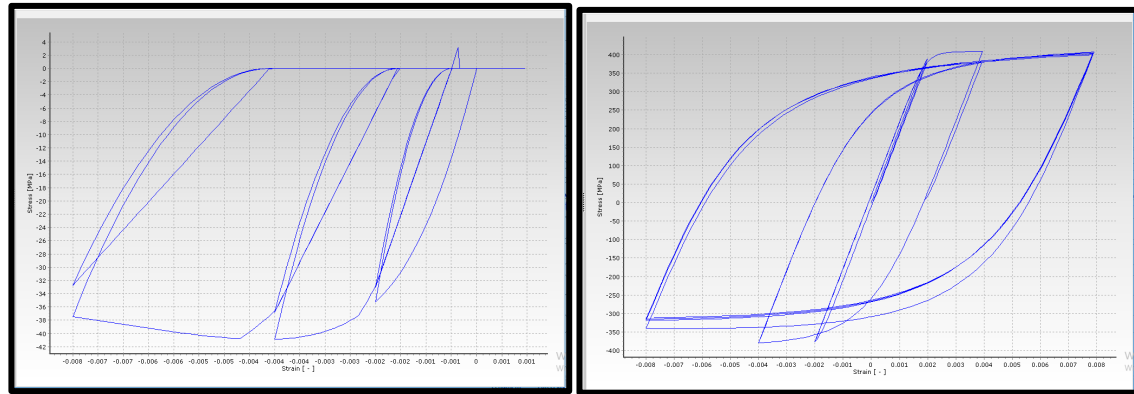


Figure 6. Fiberized section views for (a) CFST columns and (b) composite beam

Expected material strengths were used in nonlinear behavior models of steel and concrete materials used in CMRF elements. To obtain these strengths, the data in TBEC-2018 Table 5.1 were used. Accordingly, the expected material strengths predicted for the characteristic compressive strength of concrete and the characteristic yield strength of the S235 steel class are considered as  $1.3f_{ck}$  and  $1.5F_y$ , respectively. The nonlinear behavior of the steel material is represented based on a hardening of 0.005. Bilinear steel model is used for steel modelling in SeismoStruct [1] software and this is defined as “stl\_bl” material model in the software. Tensile strength is neglected in the stress-strain curve of the concrete material. In addition, the “con\_ma” model in the software was used for the non-linear behavior of the material while modelling the concrete in the SeismoStruct [1] software. Both models were developed for the cycling loading condition. The concrete material constitutive model image is shown in Figure 7a and steel material constitutive model image of the model is given in Figure 7b.



(a) (b)  
Figure 7. a) Concrete and b) steel models from SeismoStruct (2018)

Each of the nonlinear analyzes in the time domain (TH) was carried out using earthquake ground motions acting simultaneously in the horizontal plane perpendicular to each other, under the effect of a constant gravity load. While calculating the gravity load values, it has been calculated as 30% of the live load in addition to the building floor weight, that is, the fixed loads, which are effective in the earthquake. The analyzes consist of two parts. In the first stage, PO analyzes consist of 2 parts as uniformly distributed horizontal loading (ULD-PO) and triangular horizontal loading (TLD-PO). The second phase is the application phase of incremental dynamic analyzes (IDA) and TH earthquake ground motions. Earthquake ground motions consist of 8 ground motion pairs. In the selection of historical earthquake records to be used in the performance analysis using earthquake records, care was taken to select the severe earthquakes that occurred in the region. Studies in the literature show that using 7 to 20 earthquake records is sufficient for evaluation in IDA results [23-25]. When selecting earthquakes, large-scale earthquakes between the Northern Anatolian fault line and the Eastern Anatolian fault line surrounding the city of Karlıova, which is assumed to be built, were used (Figure 8). IDA and PO nonlinear analysis are frequently used by authors in reinforced concrete, steel and mixed structural systems as an important analysis methodology in the evaluation of the performance of structural systems [6, 11,12, 22, 26-31].

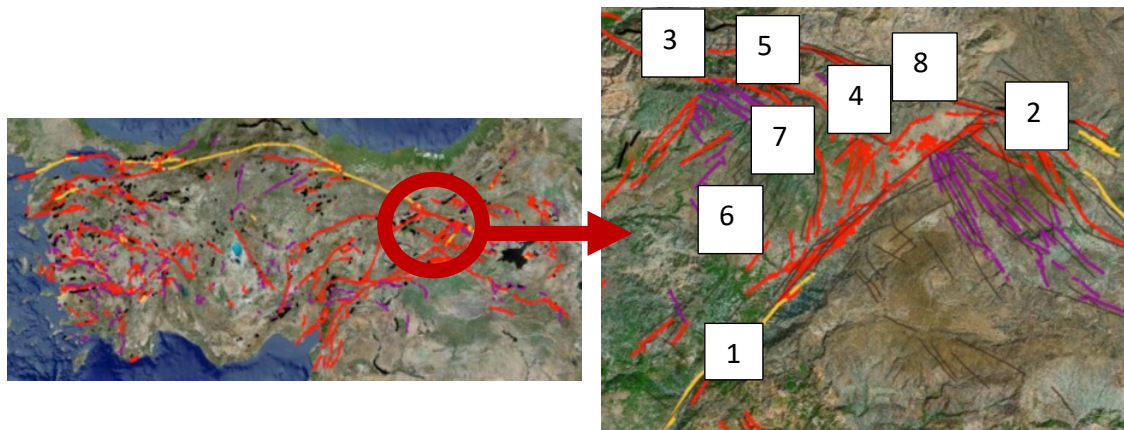


Figure 8. Selected ground motion schematic representation.

The application multipliers of the incremental effects were chosen as 0.05, 0.10, 0.20, 0.30, 0.40, 0.50, 0.60, 0.80, 1.00, 1.20, 1.40, 1.50, 1.75, 2.00, 2.30, 2.60, 2.90, 3.20, 3.50, 3.80, and 4.00. It is aimed that the total number of analyzes will be  $8 \times 2 = 16$ . In this case, the seismic demand values and other calculated parameters were determined by taking the average of 16 IDA analysis results. The characteristics of the earthquake records used in the study are given in Table 3. The information about the earthquake movements in Table 3 was taken from the AFAD ground motion database [32]. Using the existing earthquake records, each selected ground motion pair is scaled with the earthquake spectrum with a return period of 475 years, with a 10% probability of exceedance in 50 years, which is defined as a design earthquake. At the end of the analyzes carried out under these ground motion records; the structures were mutually evaluated according to the design for the targeted performance parameters.

Table 3. Properties of earthquake ground motions.

Record ID	Record Seq. #	Station ID	Event Date	Epicentral Distance (km)	Event Depth (km)	M <sub>L</sub> /M <sub>w</sub>	Component
TH-1	2183	1133	1.05.2003	11.8	6	6.6/-	East
TH-2							West
TH-3	2896	1206	25.08.2007	2.19	15.8	5.1/-	East
TH-4							West
TH-5	23	2402	13.03.1992	12.82	23	6.1/-	East
TH-6							West
TH-7	10099	1212	14.06.2020	16.2	8	-/5.7	East
TH-8							West
TH-9	24	2402	15.03.1992	45.32	29	5.4/-	East
TH-10							West
TH-11	1828	2306	25.06.2021	30.88	15.51	-/5.2	East
TH-12							West
TH-13	6027	6202	2.12.2015	37	10.66	-/5.3	East
TH-14							West
TH-15	2587	1208	14.03.2005	54.09	9.9	5.4/-	East
TH-16							West

In this study, the panel regions of the joints were modelled with the help of behavioral models originally developed by Della Corte et al. (2000) using the modified Richard-Abbott model. This model included in the SeismoStruct (2018) software includes this model, which can model all kinds of steel and composite connections (eg welded-flange bolted-web connection, extended end plate connection, recessed end plate connection, angled connection, etc.) thanks to its features. The model has increasing and decreasing parts defined by the moment-rotation relationship. The ascending and descending branches of the curve, with the presence of both positive and negative starting points with various parameters to account for load reversals (i.e. initial stiffness, strength, post-limit stiffness, shape factor, compression-related calibration coefficients, damage rate and isotropic hardening). The versatility of this type of modelling has been previously validated using experimental data, and it has been noted that the model shows excellent fit [33-36]. Also, some parameters have been calibrated to achieve greater accuracy in modeling based on the application of the component method [5, 22, 37].

### 3. Results and Discussion

The response of CMRFs because of ULD-PO and TLD-PO analysis is shown in Fig. 7. In the graphs given, the horizontal axis is the ratio of the roof displacement to the building height, and the vertical axis is the ratio of the base shear to the building weight. In 5-storey CMRFs, IDA analysis presents a behavior that lies between the first-mode dominant response and the higher-mode response. However, on the other hand, the IDA results obtained in 10-, 15- and 20-storey structures are parallel to the ULD-PO results, so it can be said that higher modes dominate in these structures [11, 16, 38]. The IDA was performed by using selected TH records to obtain the seismic response of the case study CMRFs. The dynamic behavior of the structures is also plotted in Figure 9. Figure 9 and other data obtained as a result of the analyzes are also compared with the performances of structures designed with Eurocode, which have been previously examined with similar geometric properties under the relevant headings, and the results are examined.

#### 3.1. Ductility factor

When the studies in the literature are examined, it is used to express the degree of inelastic deformations that occur due to earthquake ground motion under the influence of a structural system or a horizontal load that it may be exposed to while calculating the ductility ratio [11, 12, 16, 39]. That is, the displacement ductility ratio  $\mu$  (ductility demand) can be expressed as:

$$\mu = \frac{\Delta_u}{\Delta_y} \quad (1)$$

Yield and ultimate displacement values are  $\Delta_y$  and  $\Delta_u$ , respectively, in Eqn. (1). The result of IDAs was calculated from Figure 9 and the data were calculated and plotted for the mean  $\mu$  value. For 5-, 10-, 15- and 20-story CMRF structures,  $\mu$  factors were calculated from IDA, TLD-PO and ULD-PO and are given in Figure 8. When the  $\mu$  values obtained due to IDA are examined, it is calculated as 2.23, 1.87, 2.37 and

1.96 for 5-, 10-, 15- and 20-story buildings, respectively. When the  $\mu$  results are examined, the values obtained as a result of TLD-PO are 10.35%, 6.28% and 14.46% lower for 5-, 10- and 15-storey buildings, respectively, than the values obtained from IDA. However, the  $\mu$  values obtained because of TLD-PO in the 20-story structure are 6.55% higher than the values obtained from IDA. When the  $\mu$  values obtained because of ULD-PO were examined, it was seen that they were 17.35%, 4.77% and 9.01% lower, respectively, for 5-, 10- and 15-storey structures compared to those obtained from IDA. The  $\mu$  values calculated from the IDA and the  $\mu$  values obtained due to ULD-PO in the 20-story building are 18.06% larger (Figure 10). When the results obtained are compared with the design results of Eurocode-based structures in the literature [11,12] in average 20% greater results are obtained up to the 15-storey building formation. On the other hand, up to 20% smaller values are obtained in 20-storey buildings [11, 12]. In the literature, the general curve obtained from the load-roof displacement and the parameters that can be obtained from this curve are given in Figure 11.

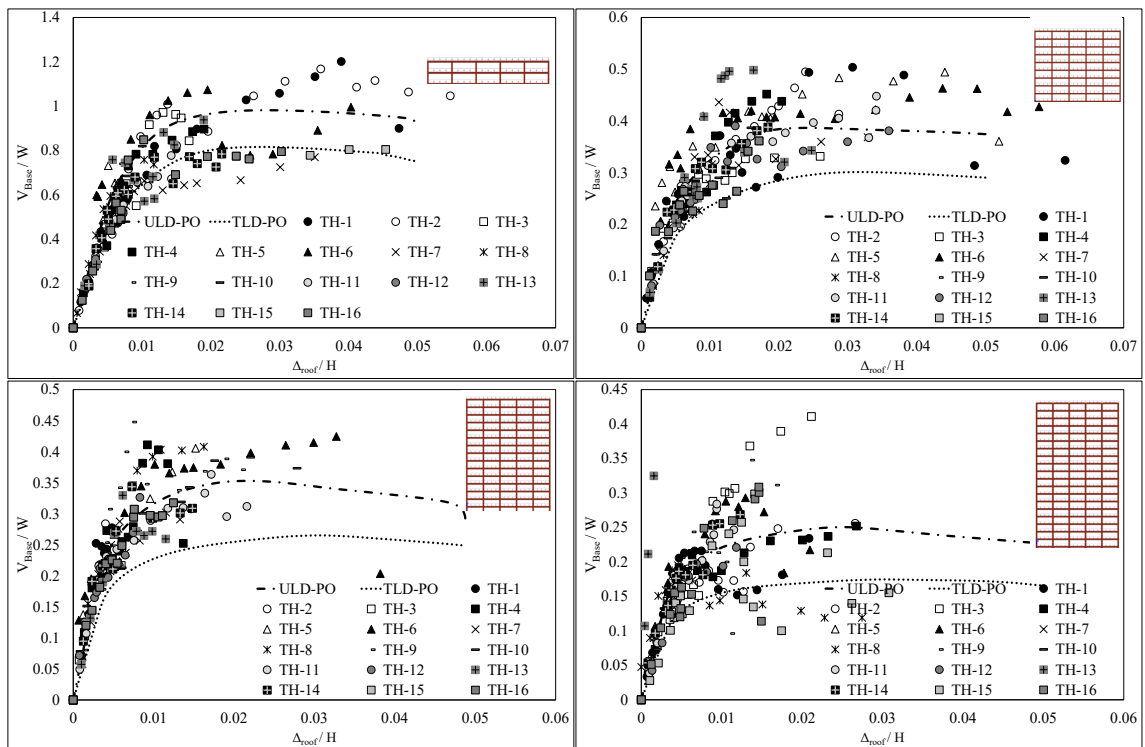


Figure 9. PO and IDA graphs for CMRF structures; 5, 10, 15, and 20 stories

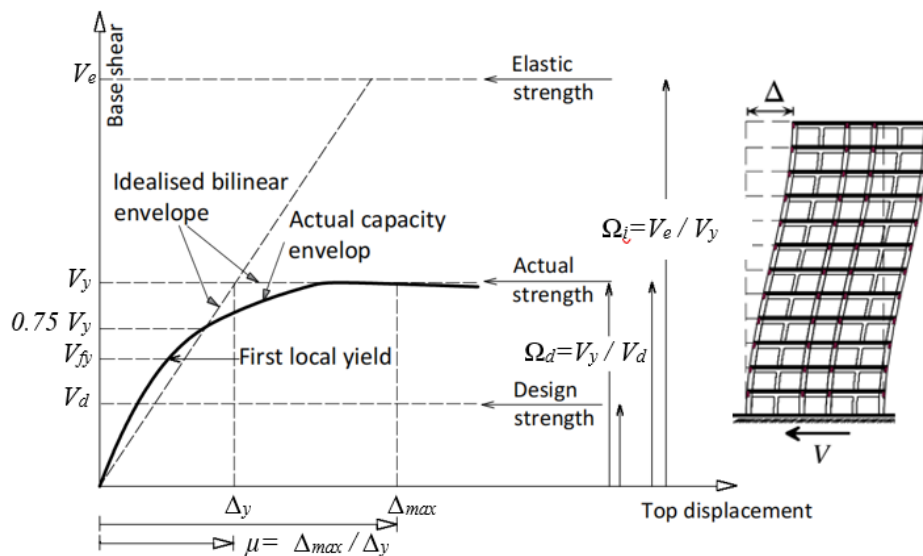


Figure 10. System view for MRF joint configuration

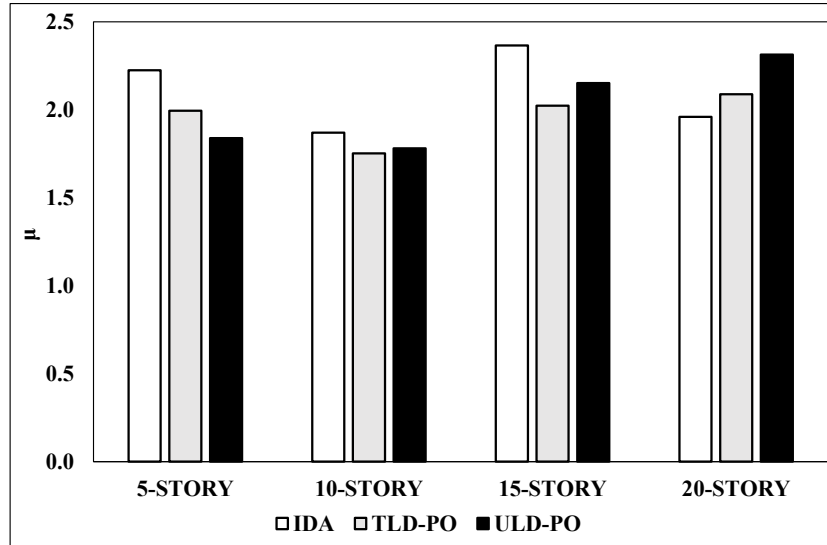


Figure 11. Ductility factor for CMRFs

### 3.2. Overstrength factor

When describing the nonlinear response of structures, the load-displacement relationship is often assumed to be elasto-plastic. Within the scope of this study, the structural extreme strength factors expressed by the following equation were calculated from the Figure 9 obtained with IDAs for each structure:

$$\Omega_d = \frac{V_y}{V_d} \quad (2)$$

Yield and design base shear values are displayed as  $V_y$  and  $V_d$ , respectively, in Eqn. (2). As a result of experimental and theoretical studies conducted by researchers for  $\Omega_d$ , an important performance parameter of the building, it has been shown that this factor plays an important role in protecting buildings from collapse in the face of severe earthquakes [40-42]. It has been reported in the literature that this factor for steel and reinforced concrete structures varies between 1.8 and 6.5 for long-term and short-term structures [40]. The IDA results in this study showed that the  $\Omega_d$  factors of CMRFs reached 7.22, 6.63, 6.75 and 6.07 in 5-, 10-, 15- and 20-story structures, respectively. The  $\Omega_d$  factors obtained from TLD-PO analyzes are 3.29% and 1.26% lower for 10- and 15-storey buildings, respectively, than those obtained from IDA. The  $\Omega_d$  factor for TLD-PO in 5- and 20-story structure is 13.61% and 2.51% larger than the values obtained from IDA. For ULD-PO it is 5.63%, 28.15%, 28.28% and 27.85% lower than the  $\Omega_d$  factors calculated from IDA for 5-, 10-, 15- and 20-story buildings, respectively (Figure 11).

Although the results obtained with the extreme hardness factor show an increase with the increasing coefficient compared to the results obtained by Etili and Güneysi [11, 12] with the Eurocode-based design, 3-33% larger results are obtained. The biggest difference is seen in buildings with 10- and 20-story [11, 12].

### 3.3. Inherent overstrength factor

Elnashai and Mwafy [43, 44] recently suggested a measure of response termed 'inherent overstrength factor. Inherent overstrength factor ( $\Omega_i$ ) is formulated as below;

$$\Omega_i = \frac{V_y}{V_e} \quad (3)$$

Yield and elastic base shear values are given as  $V_y$  and  $V_e$ , respectively, in Eqn. (3). The suggested measure of response  $\Omega_i$  reflects the reserve strength and the anticipated behavior of the structure under the design earthquake. Clearly, in the case of  $\Omega_i \geq 1.0$ , the global response will be almost elastic under the design earthquake, reflecting the high overstrength of the structure. If  $\Omega_i < 1.0$ , the difference between the value of  $\Omega_i$  and unity is an indication of the ratio of the forces that are imposed on the

structure in the post-elastic range [40]. When the values obtained within the scope of the study were examined, the values of the  $\Omega_i$  parameter were obtained as 0.93, 0.84, 0.85 and 0.76 from the IDA results for the 5-, 10-, 15- and 20-story CMRF, respectively (Figure 12). These values show that the structures can withstand earthquakes with inelastic deformations. Considering the analyzes with TLD-PO, the calculated  $\Omega_i$  values were 13.61% and 2.51% higher for the 5- and 20-story CMRF, respectively, than the IDA results. On the other hand, according to the results of the analysis made with TLD-PO, the  $\Omega_i$  value in the 10- and 15-story building is 3.29% and 1.26% lower, respectively, than the values calculated by the IDA. On the other hand, the ULD-PO results are 5.63%, 28.15%, 28.28% and 27.85% smaller than the IDA results for the 5, 10, 15 and 20-story CMRF, respectively (Figure 12). The natural strength factor results show that, according to the results obtained by Etili and Güneysi [11, 12] with the Eurocode-based design, the structures designed with TBEC-2018 will absorb earthquake energy by showing a more inflexible behavior against the Eurocode-based design under design earthquakes.

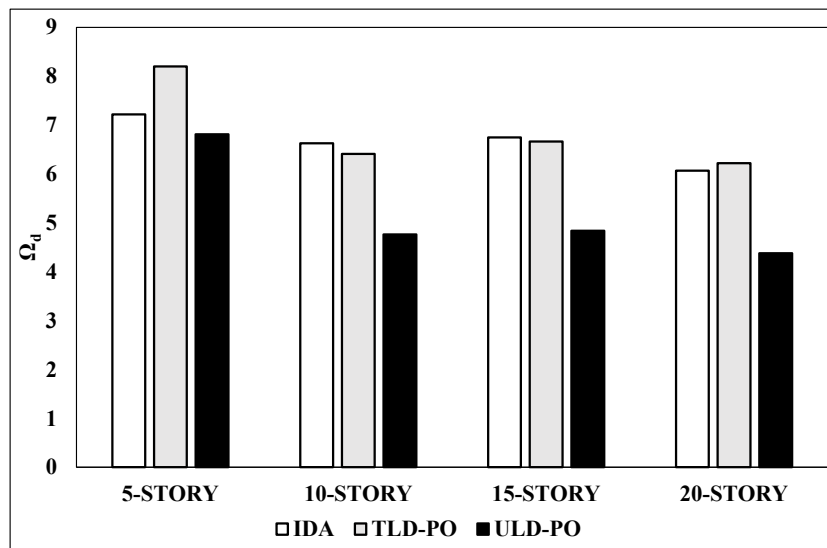


Figure 11. Overstrength factor for CMRFs

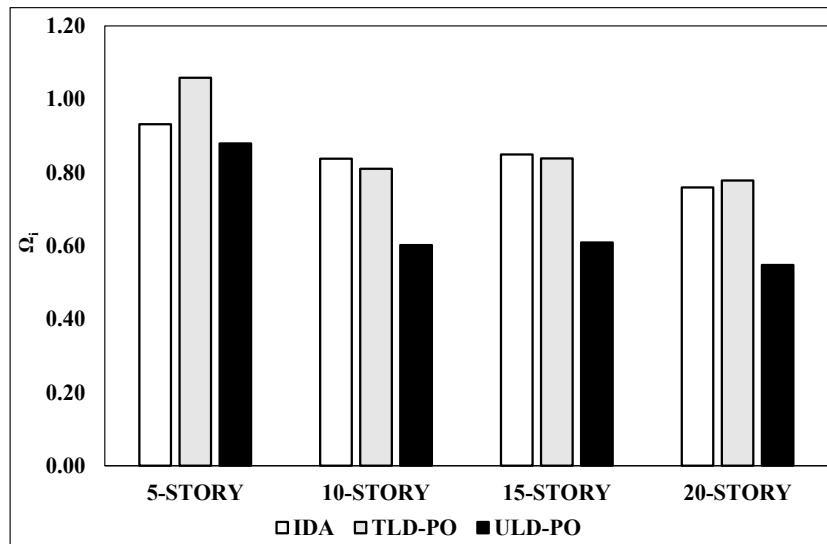


Figure 12. Inherent strength factor for CMRFs

### 3.4. Composite section capacities

In this part of the paper, the examination of the deformations in the structural elements because of the non-linear dynamic analyzes carried out in the systems formed by the CMRF structures is presented. The deformation states and definitions that occur in the mentioned structural elements are summarized in Table 4. The deformations in the CFST column sections in the CMRF system and in the sections of the composite beams formed by combining the IPE section and the solid slab are examined

within the scope of this section. During the examination, IDR (inter-story drift ratio) values were considered. Section deformations obtained during IDA, TLD-PO and ULD-PO given in Table 4 were evaluated.

Table 4. Deformation states and definitions

Deformation	Definition
BSY	In the composite beam, the steel has reached yield elongation at the outermost fiber.
CSY	In the composite column, the steel has reached yield elongation at the outermost fiber.
BSU	Steel reached its ultimate capacity in the composite beam.
CSU	Steel reached its ultimate capacity in the composite column.
BCU	Concrete reached its ultimate capacity in the composite beam.
CCU	Concrete reached its ultimate capacity in the composite column.
BCF	In the composite beam, the concrete converged to the elongation at crushing limit.

When the results of IDA, TLD-PO and ULD-PO analyzes are examined, the deformation limits of CSY, CSU and CCU in CFST elements in CMRF systems are examined, and the limit states of BSY, BSU, BCU and BCF deformations in composite beams are examined. In the IDA analysis, when the IDR value reaches 0.0072, 0.006, 0.0048 and 0.0049 in 5-, 10-, 15- and 20-story structures, respectively, the BSY deformation in composite beams is in the limit values. On the other hand, the IDR value at which BSY deformations occur in ULD-PO analyzes is 16%, 7%, 9% and 12% smaller, respectively, than the values calculated with IDA for 5-, 10-, 15- and 20-story structures. In addition, IDR values at which BSY deformations occur in TLD-PO analyzes are 17%, 3%, 5% and 11% smaller, respectively, than the values calculated with IDA for 5-, 10-, 15- and 20-storey structures. The IDR values at which BSU deformation occurred were calculated as 0.0269, 0.0324, 0.0252 and 0.0234 for 5-, 10-, 15- and 20-storey structures, respectively, from the IDA results. Therefore, the results obtained show that similar deformations are observed for TLD-PO and ULD-PO at smaller IDR values for BSY than the IDR values obtained with IDA. In ULD-PO analyzes, the IDR value at which BSU deformations occurred was 35%, 7%, 9% and 16% greater than the values calculated by IDA for 5-, 10-, 15- and 20-storey structures, respectively. In TLD-PO analysis, the IDR value at which BSU deformations occur in 5-, 10-, 15- and 20-story structures was 28%, 8%, 11% and 16% larger than the values calculated by IDA, respectively. Therefore, the results obtained show that similar deformations are observed with TLD-PO and ULD-PO at larger IDR values for BSU than the IDR values obtained with IDA. When the BCU deformation occurring in the reinforced concrete parts of the composite beams was examined, it was observed that the IDR value reached 0.0169, 0.0177, 0.0121 and 0.0107, respectively, in the 5-, 10-, 15- and 20-storey structures. On the other hand, the IDR value at which this deformation occurs in ULD-PO analyzes is 12%, 9% and 2% less, respectively, than the values calculated with IDA for 5-, 10-, and 15-storey structures. However, in a 20-story structure, it is 9% larger. In TLD-PO analyzes, the IDR value at which this deformation occurs is 5% and 6% smaller, respectively, than the values calculated by IDA for 5- and 10-storey structures. Also, while almost the same IDR value is calculated for a 15-storey building, it is 11% greater than the IDR calculated with IDA for 20-storey buildings. In the IDA analyzes, the final deformation BCF of the reinforced concrete part of the composite beams was observed when the IDR value reached 0.278, 0.0294, 0.021 and 0.0191 in 5-, 10-, 15- and 20-story structures, respectively. On the other hand, the IDR value at which this deformation occurs in ULD-PO analyzes is 19%, 16%, 13% and 5% smaller, respectively, than the IDR values calculated with IDA for 5-, 10-, 15- and 20-storey structures. In addition, in TLD-PO analyzes, the IDR value at which this deformation occurs is 11%, 13%, 10% and 4% less, respectively, than the values calculated with IDA for 5-, 10-, 15- and 20-storey structures. Therefore, the results obtained show that similar deformations are observed with TLD-PO and ULD-PO at smaller IDR values for BCF than the IDR values obtained with IDA (Figure 13).

Deformations occurring in CFSTs were observed as CSY, CSU and CCU. CSY deformation in CFST is at the limit values when IDR value reaches 0.0117, 0.0157, 0.0171 and 0.0232 values for 5-, 10-, 15- and 20-story structures, respectively, in IDA analyzes. On the other hand, the IDR value at which CSY deformations occur in ULD-PO analyzes is 5%, 13%, 15% and 20% higher, respectively, than the IDR values calculated with IDA for 5-, 10-, 15- and 20-storey structures. In addition, the IDR value at which CSY deformations occur in TLD-PO analyzes is 22%, 50%, 66% and 83% higher, respectively, than the IDR values calculated with IDA for 5-, 10-, 15- and 20-storey structures. Therefore, the results obtained show that similar deformations are observed for TLD-PO and ULD-PO at smaller IDR values for CSY than the IDR values obtained with IDA. The IDR values at which CSU deformation occurred were calculated as 0.0466, 0.0556 and 0.0545 for 5-, 10- and 15-storey structures, respectively, from the IDA results. On the other hand, there is no IDR value in which the values of this deformation are seen in the 20-story CMRF. In ULD-PO analyzes, the IDR value at which CSU deformations occur is 18%, 14% and

6% smaller, respectively, than the values calculated with IDA for 5-, 10- and 15-storey structures. The structures in which CSU deformations occur in TLD-PO analyzes are only 5- and 15-storey structures. For this analysis method, the IDR value is 5% smaller than the values calculated with IDA for 5-storey buildings, while it is 25% higher for 15-storey buildings. The IDR values at which CCU deformation occurred were calculated as 0.0307, 0.0357 and 0.0355 for 5-, 10-, and 15-storey structures, respectively, from the IDA results. In 20-story CMRF, this deformation was not observed in the IDR values calculated as a result of TLD-PO. The IDR value at which CSU deformations occur in ULD-PO analyzes is 11% and 5% smaller than the values calculated with IDA for 5- and 10-storey structures, respectively. In addition, in the ULD-PO analysis, CSU deformations occurred at a 3% higher IDR value than the IDR values obtained in the 15-storey structure. In addition, the CCU deformation of the 20-story structure was observed only in the analyzes with ULP-PO and the IDR value was calculated as 0.058. In TLD-PO analysis, CCU deformations in 5, 10, and 15-storey structures were 6%, 25%, and 44% greater than the values calculated by IDA (Figure 13). On the other hand, in a project-based study conducted by Güneyisi [15], it is seen that the deformations obtained as a result of IDA in the structures obtained with the Eurocode have more limited deformations than the structures produced with TBEC-2018. In both studies, inelastic deformation occurs rarely in columns in 5-story structures, but inelastic deformation occurs more frequently in 5-, 10-, 15- and 20-storey beams.

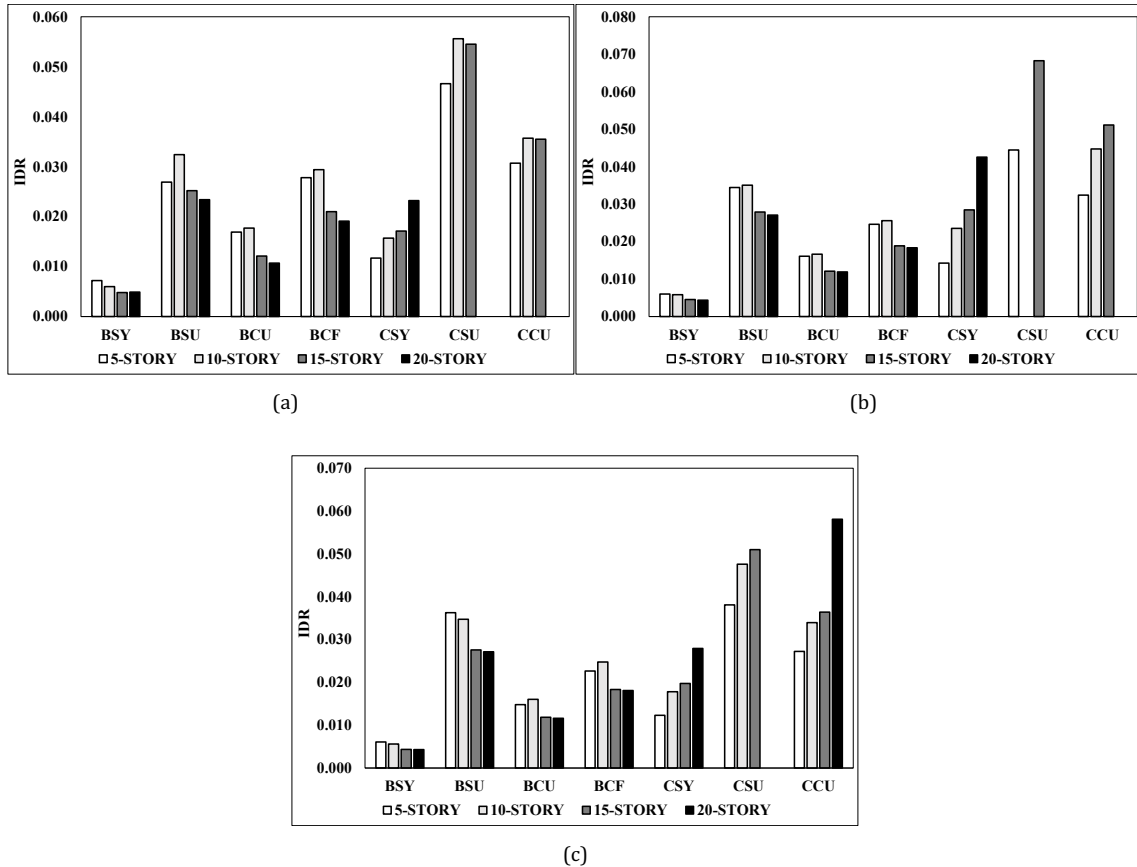


Figure 13. Section deformation variation with IDR for a) IDA, b) TLD-PO, and c) ULD-PO

#### 4. Conclusions

In this study, the structures designed according to TDCSS-2016 and TBEC-2018 design codes were evaluated using deformations in the sections of the elements and various performance parameters, assuming that they were built on soils containing moderately frequent sand and modified stones (*ZC* group soil). For this, static pushover analysis and incremental dynamic analysis were performed. PO analysis with two different lateral load models. When the data obtained are examined, the following conclusions can be reached:

- When the  $\mu$  values are examined, the obtained values are greater than 1.7. This shows that CMRF structures can adequately absorb earthquake effects thanks to horizontal displacements in a ductile manner. These values are also supported by other studies in the literature [11,12,16].

- In addition, when the  $\mu$  values obtained as a result of the IDA are examined, it is seen that the IDA results in medium and high-rise buildings are on average 5% higher than TLD-PO and ULD-PO.
- The  $\Omega_d$  parameter calculated by using IDA analyzes using selected regional earthquakes for the buildings designed as TDCSS-2016 and TBEC-2018 and for the buildings designed as CMRF was obtained as 6.07 at least. In addition, the lowest score in PO analyzes is 4.38. However, considering that the behavior factor is obtained when the  $\mu$  values are multiplied by the  $\Omega_d$  parameter, the lowest values to be obtained for the IDA and PO analyzes are 11.89 and 8.48. As a result, they have higher performance factors than calculations with  $R=8$  design factor.
- When the  $\Omega_i$  values are examined, it is seen that almost all the values obtained are less than 1. In this case, structures indicate that they will absorb earthquake energy thanks to their inflexible behavior. However, this is a possible situation in earthquake situations larger than the design earthquake. Moreover, the results obtained from the  $\mu$  and  $\Omega_d$  parameters support that the structure is an economical design model.
- When the composite beams are examined according to the IDR change, it is seen that the behavior is within the elastic limits when the IDR value is 0.005. When the IDR value is above 0.02, the plastic behavior dominates in the composite beams. However, this situation emerges as a decreasing IDR value as the number of floors increases. In addition, plastic behaviors observed in concrete occur when the IDR value approaches 0.015 in beam sections.
- In addition, when CFST columns are examined according to IDR change, it can be said that when the IDR value is 0.01, the behavior is within elastic limits and then plastic deformations occur. Plastic behavior is common in CFST columns when the IDR value is above 0.03. However, this situation emerges as an increasing IDR value as the number of stories increases.

## Conflict of Interest Statement

The authors declare that there is no conflict of interest.

## References

- [1] SeismoSoft, "SeismoStruct: A computer software for static and dynamic nonlinear analysis of framed structures," SeismoSoft.com, 2018. [Online]. Available: [www.seismosoft.com](http://www.seismosoft.com). [Accessed: Jan. 12, 2023].
- [2] A. Y. Elghazouli, "Assessment of European seismic design procedures for steel framed structures," *Bulletin of Earthquake Engineering*, vol. 8, pp. 65-89, 2009. doi:10.1007/s10518-009-9125-6
- [3] N. E. Shanmugam and B. Lakshmi, "State of the art report on steel-concrete composite columns," *Journal of Constructional Steel Research*, vol. 57, pp. 1041-1080, 2001. doi:10.1016/S0143-974X(01)00021-9
- [4] M. Shams and M. A. Saadeghvaziri, "State of the art of concrete-filled steel tubular columns," *ACI Structural Journal*, vol. 94, pp. 558-571, 1997. doi:10.14359/505
- [5] S. Etili, "Analytical Evaluation of Behavior of Composite Columns Under Axial Load," *International Journal of Pure and Applied Sciences*, vol. 7, no. 3, pp. 526-536. 2021. doi:10.29132/ijpas.991166
- [6] S. Etili, "Parametric Analysis of the Performance of Steel-Concrete Composite Structures Designed with TBDY 2018," *International Journal of Innovative Engineering Applications*, vol. 6, no. 1, pp. 7-16, 2022. doi:10.46460/ijiea.1029942
- [7] L. H. Han, W. Li and R. Bjorhovde, "Developments and advanced applications of concrete-filled steel tubular (CFST) structures: members," *Journal of Constructional Steel Research*, vol. 100, pp. 211-228. 2014. doi:10.1016/j.jcsr.2014.04.016
- [8] M. D. Denavit, J. F. Hajjar, T. Perea and R. T. Leon, "Stability Analysis and Design of Composite Structures," *Journal of Structural Engineering (United States)*, vol.142, pp. 1-12, 2016. doi:10.1061/(ASCE)ST.1943-541X.0001434
- [9] M. D. Denavit, J. F. Hajjar, T. Perea and R. T. Leon, "Seismic performance factors for moment frames with steel-concrete composite columns and steel beams," *Earthquake Engineering & Structural Dynamics*, vol. 45, pp. 1685-1703, 2016. doi:10.1002/eqe.2737
- [10] M. D. Denavit and J. F. Hajjar, "Nonlinear seismic analysis of circular concrete-filled steel tube members and frames," *Journal of Structural Engineering*, vol.138, pp. 1089-1098, 2012. doi:10.1061/(ASCE)ST.1943-541X.0000544

- [11] S. Etili and E. M. Güneyisi, "Seismic performance evaluation of regular and irregular composite moment resisting frames," *Latin American Journal of Solids and Structures*, vol. 17, pp. 1-22, 2020. doi:10.1590/1679-78255969
- [12] S. Etili and E. M. Güneyisi, "Assessment of Seismic Behavior Factor of Code-Designed Steel-Concrete Composite Buildings," *Arabian Journal for Science and Engineering*, vol. 46, pp. 4271-4292, 2021. doi:10.1007/s13369-020-04913-9
- [13] A. Zona, M. Barbato and J.P.Conte, "Nonlinear Seismic Response Analysis of Steel-Concrete Composite Frames," *Journal of Structural Engineering*, vol. 134, pp. 986-997, 2008. doi:10.1061/(ASCE)0733-9445
- [14] C. Vatansever and Y.E. Şimşek, "Design and nonlinear time history analysis of a multi-story building with concrete filled composite columns and steel beams," *Pamukkale University Journal of Engineering Sciences – PAJES*, vol. 27, no. 3, pp. 264–273, 2021. doi:10.5505/pajes.2020.91043
- [15] E. M. Güneyisi and S. Etili, "Investigation of the Effect of Diagonal Eccentricity on Behavior of Braced Composite Structures Under the Impact of Near and Far-field Earthquakes," TUBİTAK. PROJECT NO, 2021.
- [16] S. Etili, and E. M. Güneyisi, "Response of steel buildings under near and far field earthquakes," *Journal of Civil Engineering Beyond Limits*, vol. 1, pp. 24–30, 2020. doi:10.36937/cebel.2020.002.004
- [17] Environment And Urban Ministry of Turkey, "Regulation on Design, Calculation and Construction Principles of Steel Structures," Turkey, 2016.
- [18] TBEC-2018, "Turkey Disaster and Emergency Management Presidency: Turkey Building Earthquake Regulation," Turkey, 2018.
- [19] Turkey Disaster and Emergency Management Presidency, "Turkey Earthquake Hazard Maps," Available: <https://tdth.afad.gov.tr/>.
- [20] TS-498, "Yapı elemanlarının boyutlandırılmasında alınacak yüklerin hesap değerleri," Türk Stand. Enstitüsü, 2007.
- [21] S. Etili and E. M. Güneyisi, "Effect of Using Eccentric Braces with Different Link Lengths on the Seismic Demand of CFST Column-Composite Beam Frames Subjected to Near-Field and Far-Field Earthquakes," *Iranian Journal of Science and Technology*, 2022. doi:10.1007/s40996-022-00994-8
- [22] S. Etili and E. M. Güneyisi, "Effect of nonlinear modeling approaches used for composite elements on seismic behavior of composite framed buildings," *Sâdhânâ*, vol. 47, 2022. doi:10.1007/s12046-022-01871-w
- [23] A. Y. Elghazouli, J. M. Castro and B. A. Izzuddin, "Seismic performance of composite moment-resisting frames," *Engineering Structures*, vol. 30, no. 7, pp. 1802-1819, 2008. doi:10.1016/j.engstruct.2007.12.004
- [24] D. Vamvatsikos, *Seismic performance, capacity and reliability of structures as seen through incremental dynamic analysis*, Stanford University, 2002.
- [25] M. Ferraioli, A. Lavino and A. Mandara, "Behaviour factor of code-designed steel moment-resisting frames," *International journal of steel structures*. Vol. 14, pp. 243-254, 2014.
- [26] N. Fanaie and R. Sheykhi, "Seismic Behaviour Assessment of Eccentrically Split-X Braced Frames," *Scientia Iranica*, vol. 28, pp. 65-84, 2019. doi:10.24200/sci.2019.50655.1804
- [27] A. Seyedkazemi and F. Rofooei, "Comparison of Static Pushover Analysis and IDA-Based Probabilistic Methods in Assessing the Seismic Performance Factors of Diagrid Structures," *Scientia Iranica*, vol. 28, pp. 124-137, 2019. doi:10.24200/sci.2019.51555.2250
- [28] M. Zanjanchi and M. Mofid, "On the assessment of MIDA method for mid-rise steel structures with non-symmetrical plan" *Sci. Iran.*, vol. 26, pp. 2703-2711, 2019. doi:10.24200/sci.2019.21356
- [29] A. Bakhshi and H. Soltanieh, "Development of fragility curves for existing residential steel buildings with concentrically braced frames," *Scientia Iranica*, vol. 26, pp. 2212-2228, 2019. doi:10.24200/sci.2019.21498
- [30] M. Sabouniaghdam, E. Mohammadi Dehcheshmeh, P. Safari and V.Broujerdian, "Probabilistic collapse assessment of steel frame structures considering the effects of soil-structure interaction and height," *Scientia Iranica*, vol. 29, no. 6, pp. 2979-2994, 2022. doi:10.24200/sci.2022.58707.5860
- [31] M. Maddahi, M. Gerami and H. Naderpour, "Effect of structural uncertainties on seismic performance of moment frame rehabilitated with steel shear wall," *Scientia Iranica*, vol. 28, no. 4, pp. 2010-2022, 2020. doi:10.24200/sci.2020.54252.3668
- [32] TADAS, "Turkey Acceleration Database and Analysis System (TADAS)," [mdsoft.com.tr](http://www.mdsoft.com.tr), [Online]. Available: [http://www.mdsoft.com.tr/Pages/Product\\_EqAcc](http://www.mdsoft.com.tr/Pages/Product_EqAcc). [Accessed: Jul. 12, 2023].
- [33] G. Della Corte, G. De Matteis and R. Landolfo, "Influence of connection modelling on seismic response of moment resisting steel frames," *Moment resistant connections of steel frames in seismic areas - Design and reliability*, E&FN SPON London, pp. 485-

512, 2000. doi:10.1017/CBO9781107415324.004

[34] R. Simoes, L. S. da Silva, P. J. S. Cruz, "Cyclic behaviour of end-plate beam-to-column composite joints," *Steel and Composite Structures*, vol. 1, pp. 355-376, 2001. doi:10.12989/scs.2001.1.3.355

[35] M. F. B. Shamsudin, "Analytical Tool for Modeling the Cyclic Behaviour of Extended End-Plate," Master Thesis, University of Coimbra, Coimbra, Portugal, 2014.

[36] P. Nogueiro, L.S. Da Silva, R. Bento and R. Simões, "Calibration of model parameters for the cyclic response of end-plate beam-to-column steel-concrete composite joints," *Steel and Composite Structures*, vol. 9, pp. 39-58, 2009. doi:10.12989/scs.2009.9.1.039

[37] J. P. Jaspart and K. Weynand, *Design of Joints in Steel and Composite Structures*, ECCS and Ernst & Sohn, 2016.

[38] D. Vamvatsikos and C. A. Cornell, "Direct estimation of the seismic demand and capacity of MDOF systems through Incremental Dynamic Analysis of an SDOF approximation," *Journal of Structural Engineering*, vol. 131, pp. 589-599, 2005. doi:10.1061/(ASCE)0733-9445

[39] E. Miranda and V. V. Bertero, "Evaluation of Strength Reduction Factors for Earthquake-Resistant Design," *Earthquake Spectra*, vol. 10, pp. 357-379, 1994. doi:10.1193/1.1585778

[40] A. S. Elnashai and L. Di Sarno, *Fundamentals of Earthquake Engineering: From Source to Fragility*, 2nd Edition. John Wiley & Sons, 2015.

[41] A. Whittaker, G. Hart and C. Rojahn, "Seismic response modification factors" *Journal of Structural Engineering*, vol. 125, pp. 438-444, 1999.

[42] A. S. Elnashai and A. M. Mwafy, "Overstrength and force reduction factors of multistorey reinforced-concrete buildings," *The Structural Design of Tall Buildings*, vol. 11, no. 5, pp. 329-351, 2002.

[43] A. M. Mwafy and A. S. Elnashai, "Static pushover versus dynamic collapse analysis of RC buildings," *Engineering Structures*, vol. 23, no. 5, pp. 407-424, 2001. doi:10.1016/S0141-0296(00)00068-7

[44] A. M. Mwafy, "Seismic performance of code-designed RC buildings," PhD Thesis, Technology and Medicine University of London, London, 2001.

This is an open access article under the CC-BY license

